International Journal of Power Electronics and Drive System (IJPEDS)
Vol. 4, No. 3, September 2014, pp. 343~355
ISSN: 2088-8694

Review of the UPFC Different Models in Recent Years

Mahmoud Zadehbagheri, Rahim Ildarabadi, Majid Baghaei Nejad
Faculty of Electrical, Department of Electrical Engineering, Hakim Sabzevari University, Sabzevar, Iran

Article Info

Article history:

Received Mar 14, 2014
Revised Apr 8, 2014
Accepted Apr 25, 2014

Keyword:

Reactive Power
Steady-state
Transmission Line
Unified Power Flow Controller
Voltage Control

ABSTRACT

Unified Power Flow Controller (UPFC) is one of the most intriguing and, potentially, the most versatile classes of Flexible AC Transmission Systems (FACTS) devices. The UPFC is a device which can control simultaneously tree parameters line impedance, voltage, phase angle and dynamic compensation of AC power system. In order to analyze its true effects on power systems, it is important to model its constraints, due to various ratings and operating limits. This paper reviews on the different models of UPFC used in recent years and gives sets of information for each model of the UPFC in AC transmission. Then the different models are compared and features of each model are examined.

Corresponding Author:

Mahmoud Zadehbagheri,
Departement of Electrical Engineering,
Hakim Sabzevari University,
Sabzevar, Iran.
Email: mzadehbagheri@gmail.com

1. INTRODUCTION

Unified Power Flow Controller (UPFC) is considered as a powerful device of the Flexible Alternating Current Transmission Systems (FACTS) family, where it has both a shunt and a series controller inside its frame. Therefore UPFC has the ability to do both of Static VAR Compensator (SVC) and Static Synchronous Series Compensator (SSSC) performance simultaneously [1]. UPFC allows not only the combined application of phase angle control with controllable series reactive compensations and voltage regulation, but also the real-time transition from one selected compensation mode into another one to damp oscillations and to handle particular system contingencies more effectively [2]. The UPFC allows simultaneous control of active power flow, reactive power flow, and voltage magnitude at the UPFC terminals. Alternatively, the controller may be set to control one or more of these parameters in any combination or to control none of them [3]. In fact, there are three types of FACTS modeling [7]: electro magnetic models for detailed equipment level investigation; dynamic models for stability analysis; and steady-state models for steady state operation evaluation. In recent years, the use of the UPFC for different aims has received increased attention. This paper presents different model of UPFC in recent years.

2. DIFFERENT MODELS

Miller [4] talks about the dynamic behavior of two different flexible ac transmission system devices; the Interline Power-flow Controller (IPFC) and the Unified power-flow Controller (UPFC) in a benchmark system. A small model of the IPFC is validated via electromagnetic transients (EMT) simulation using a 12-bus network which can model multiple oscillatory modes. The UPFC consists of a shunt VSC and a series VSC connected via a common dc bus which includes a dc capacitor for ripple control. The shunt VSC provides voltage support to the connected bus .The series VSC has the ability to precisely control power flow

in the line. In the IPFC the two VSC converters are both inserted in series with two different lines and share a common dc bus. Hence, they have the capability to precisely control power flow in two different transmission lines (Figure 1). By using this model, the damping capabilities of the IPFC and UPFC are compared and some results are obtained. Installing an IPFC or UPFC in constant power control mode for the series branch has the same effect as disconnecting the transmission line containing the series branch. This network structure change may be used to improve system damping without requiring the design of a tuned feedback controller. Theoretically, still there is the possibility of existing poorly damped modes in the changed network; if there is such a mode, a damping controller which can modulate the power references of the FACTS device can be introduced. The IPFC has two series branches, while the UPFC has a single series branch so; the IPFC permits more opportunities for network segmentation. Consequently, the IPFC has potential for greater damping improvement and also improving the system's dynamic performance. Reference [5] is aimed at finding the optimal UPFC control mode and settings to improve the composite reliability of power systems when all UPFC components are available. The proposed approach will minimize ESRAC for improving the system reliability. A selected set of contingencies are analyzed and the optimal power flow (OPF) is used to minimize RAC and calculate the optimal UPFC injections and the sensitivity of RAC to UPFC injections. The results of contingency analyses are used to calculate post-contingency injections of UPFC and to estimate the ESRAC associated with control modes and settings. The optimal UPFC control mode and settings are obtained by solving the proposed mixed-integer nonlinear optimization problem. The two-source power injection model shown in Figure 2 is used to represent the UPFC in optimal power flow studies. In this model, parallel source (PS) and series source (SS) are connected to PB and SB, respectively, so that the total real power injection of PS and SS is zero:

$$P_{PS} = P_{SS} \tag{1}$$

In Figure 2, once the three independent injections of PS and SS (i.e.,$P_{SS}, Q_{SS}\ and\ Q_{PS}$) are known, the voltage and current of series and parallel inverters in Figure 1 are calculated as follows:

$$\overline{I_{SB}} = \frac{P_{SS} - JQ_{SS}}{\bar{V}_{SR}} \tag{2}$$

$$\overline{I_{PB}} = \frac{P_{PS} - JQ_{PS}}{\overline{V_{PB}}} \tag{3}$$

$$V_{SI}\angle\theta_{SI} = \overline{V_{SB}} - \overline{V_{PB}} - jX_{ST}\overline{I_{SB}} \tag{4}$$

$$V_{PI}\angle\theta_{PI} = \overline{V_{PB}} + jX_{PT}(\overline{I_{SB}} - \overline{I_{PB}}\ ) \tag{5}$$

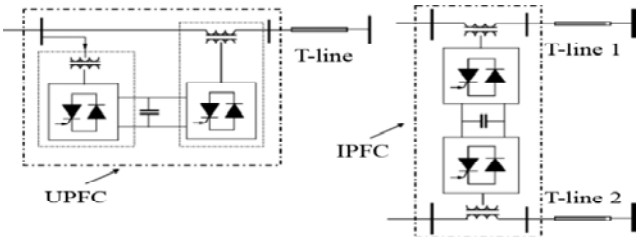

Figure 1. Converter-based FACTS

Control modes associated with series and parallel inverters are also considered for PS and SS, respectively, as:

$$mode\ \text{series} = \begin{cases} 1 & \textbf{Power Flow control Mode (PFM)} \\ 2 & \textbf{Voltage Control Mode (VCM)} \\ 3 & \textbf{Voltage Injection Mode (VIM)} \end{cases} \tag{6}$$

$$mode\ parallel = \begin{cases} 1 & \textbf{Reactive Control Mode (RCM)} \\ 2 & \textbf{Voltage Control Mode (VCM)} \end{cases} \tag{7}$$

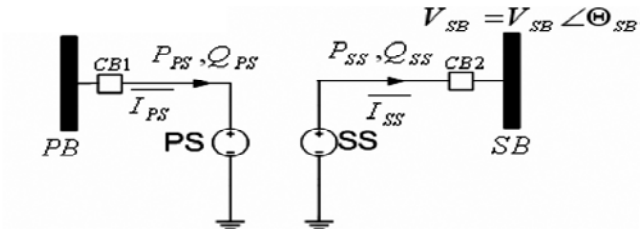

Figure 2. Two-source power injection model for UPFC

The two-state up/down model is used for reliability studies. The proposed method finds the optimal control mode and settings when the UPFC is in the up state. The method can further be extended to include other operating states of UPFCs. In Reference [6] the UPFC is connected at the midpoint of the Transmission line. The basic components of the UPFC are two voltage source inverters (VSIs) sharing a common DC storage capacitor, and connected to the system through coupling transformers. One VSI is connected in shunt to the transmission system via a shunt transformer, whereas the other one is connected in series through a series transformer (Figure 3).

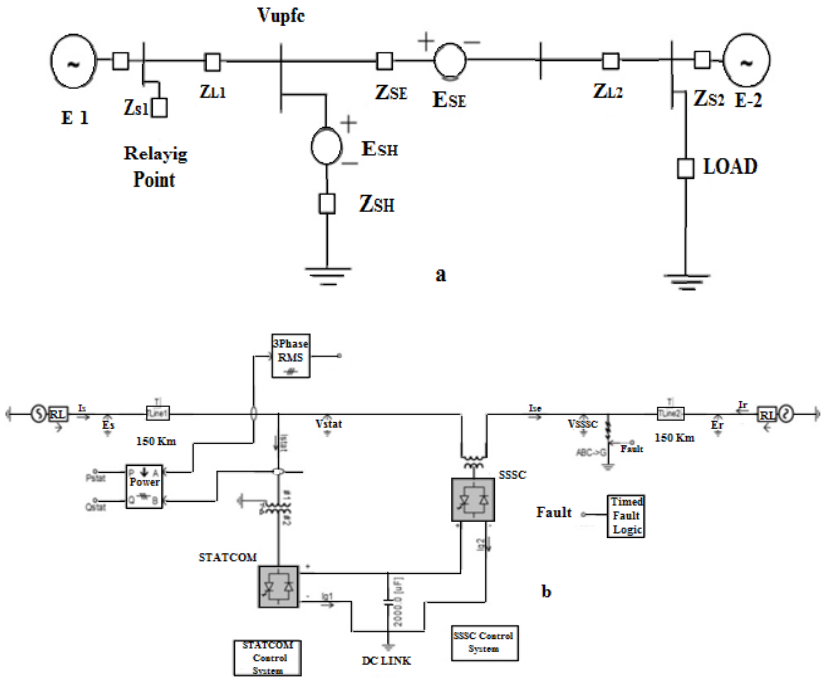

Figure 3. UPFC based transmission system, a) Transmission system with UPFC
b) UPFC-based transmission line model

The UPFC control system is divided into two parts, STATCOM control and SSSC control. The STATCOM is controlled to operate the VSI for reactive power generation at the connecting point voltage V_{ref}. The voltages at the connecting points are sent to the phase locked- loop (PLL) to calculate the reference angle, which is synchronized to the reference phase voltage. The currents are decomposed into the direct and quadrature components, Id and Iq by a d-q transformation using the PLL angle as reference. The magnitude of the positive sequence component of the connecting point voltage is compared with V_{ref} and the error is passed through the PI controller to generate I_{qref}. The reactive part of the shunt current is compared with I_{qref} and the error is passed through the PI controller to obtain the relative phase angle of the inverter voltage with respect to the reference phase voltage. This phase angle and the PLL signal are fed to the STATCOM firing circuit to generate the desired pulse for the VSI. The series injected voltage is determined by the closed loop control system to ensure that the desired active and reactive power flow occurs despite power system

changes. The desired P $_{ref}$ and Q $_{ref}$ are compared with the measured active and reactive power flow in the transmission line, and the error is passed through the PI controller to derive the direct and quadrature components of the series inverter voltage, V $_{dref}$ and V $_{qref}$. Thus, the series injected voltage and phase angle can be found out from the rectangular to polar conversion of the V $_{dref}$ and V $_{qref}$. The dead angle (found out from the inverter voltage and DC link voltage), phase angle and the PLL signal are fed to the firing circuit to generate the desired pulse for the SSSC VSI.

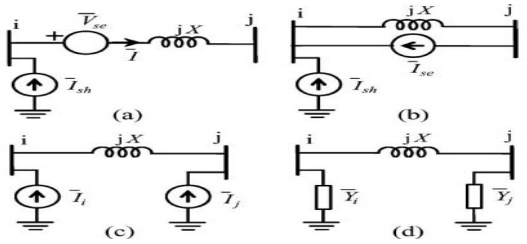

Figure 4. Successive representation of a UPFC and its associated line

The dynamic model of a UPFC is used by a large number of researchers for dynamic analysis of a power system [8]-[13]. The UPFC and the associated transmission line are separately shown in Figure 4 where the UPFC is represented by a series voltage source$\overline{V_{se}}$ and a shunt current source$\overline{I_{sh}}$. Note that $\bar{V}_{se}$ and $\bar{I}_{sh}$are not constant but depend on the control strategy used. For simplicity, the line is first represented by only its series reactance X. The leakage reactance of the series injection transformer (if any) can be included in$X$. The voltage source V_{se} in series with can be represented by a current source $\overline{I_{sh}}$in parallel with X as shown in Figure 3(b).

$$\overline{I_{se}} = {V_{se}}/{jX} \tag{8}$$

Without loss of generality, the current source I_{se}between buses $i$and $j$can be replaced by two shunt current sources (at buses i and). Such an equivalent circuit is shown in Figure 3(c) where:

$$\bar{I}_i = \bar{I}_{sh} + \bar{I}_{se} \qquad and \quad \bar{I}_j = -\overline{I_{se}} \tag{9}$$

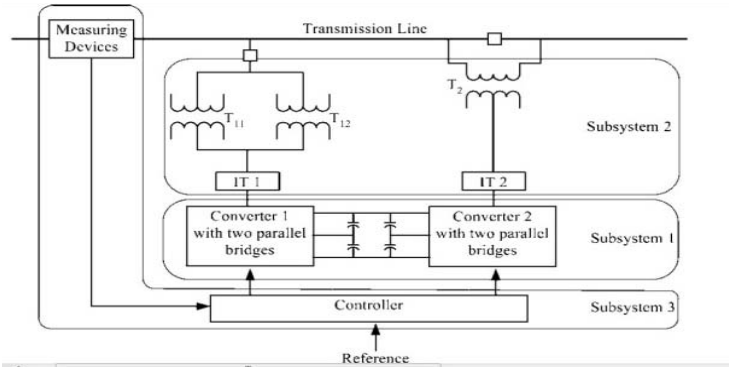

Figure 5. UPFC components and their classification into three subsystems

Figure 3(d) represents the π-circuit model of a UPFC and its associated transmission line. The UPFC model can also be used to represent an SSSC or a STATCOM by selecting appropriate values of $\overline{V_{se}}$and$\overline{I_{sh}}$. For an SSSC, it is necessary to set$\overline{I_{sh}} = 0$ and thus $\bar{I}_i$of (4) simply becomes$\overline{I_{se}}$. In this case, $\overline{V_{se}}$is kept in quadrature with the prevailing line current. However, for a STATCOM, $\overline{V_{se}}$ (and hence I_{se}) is to be set to zero. A large number of researchers [14]-[18] used the UPFC system which is classified into three subsystems: the converters and capacitor link (CL) as subsystem 1, the coupling and intermediate

transformers as subsystem 2 and the controller with the corresponding measuring equipment as subsystem 3. In order to develop a reliability model of a UPFC, the aforementioned subsystems must be modeled followed by the development of a complete reliability model of the UPFC. The world's first UPFC, which was commissioned in June 1998 at the Inez substation of American Electric Power in Kentucky, has been modified in their researches as shown in Figure 5.

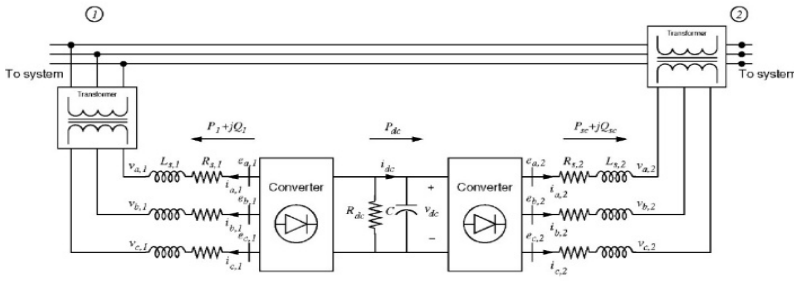

Figure 6. Unified power flow controller diagram

The actual Inez UPFC comprises two identical gate turn off (GTO) thyristor-based converters. Each converter includes multiple high-power GTO valve structures feeding an intermediate transformer. The converter output is coupled to the transmission line by a conventional main coupling transformer. To maximize the versatility of the installation, two identical main shunt transformers and a single main series transformer have been provided. With this arrangement, a number of power circuit configurations are possible. Reference [19], [20] has used another model of UPFC as shown in Figure 6. The series connected inverter injects a voltage with controllable magnitude and phase angle in series with the transmission line, thereby providing active and reactive power to the transmission line. The shunt-connected inverter provides the active power drawn by the series branch and the losses and can independently provide reactive compensation to the system. The UPFC state model is:

$$\frac{1}{\omega_S}\frac{d}{dt}i_{d1} = \frac{k_1 V_{dc}}{L_{s1}}\cos(\propto_1 + \theta_1) + \frac{\omega}{\omega_s}\, i_{q1} - \frac{R_{S1}}{L_{s1}} id_1 - \frac{V_1}{L_{s1}} cos\theta_1 \quad (10)$$

$$\frac{1}{w_s}\frac{d}{dt}i_{q1} = \frac{k_1 V_{dc}}{L_{s1}}\sin(\alpha_1 + \theta_1) - \frac{R_{S1}}{L_{s1}} i_{q1} - \frac{w}{w_s} i_{d1} - \frac{V_1}{L_{s1}}\sin(\theta_1) \quad (11)$$

$$\frac{1}{w_s}\frac{d}{dt}i_{d2} = -\frac{R_{S2}}{L_{s2}} i_{d2} + \frac{w}{w_s} i_{d2} + \frac{K_2}{L_{s2}}\cos(\alpha_2 + \theta_1)\, V_{dc} - \frac{1}{L_{s2}}(V_2 cos\theta_2 - V_1\cos(\theta_1)) \quad (12)$$

$$\frac{1}{w_s}\frac{d}{dt}i_{d2} = -\frac{R_{S2}}{L_{s2}} i_{d2} + \frac{w}{w_s} i_{d2} + \frac{K_2}{L_{s2}}\sin(\alpha_2 + \theta_1)\, V_{dc} - \frac{1}{L_{s2}}(V_2 sin\theta_2 - V_1\sin\theta_2) \quad (13)$$

$$\frac{c}{w_s}\frac{d}{dt}V_{dc} = -K_1\cos(\alpha_1 + \theta_1)\, i_{d1} - K_1\sin(\alpha_1 + \theta_1)\, i_{q1} - k_2\cos(\propto_2 + \theta_1)\, i_{d2} - k_2\sin(\alpha_2 + \theta 1 iq2 - VdcRdc \quad (14)$$

The currents id_1 and i_{q1} are the dq components of the shunt current. The currents $i_{d2}$and$i_{q_2}$are the dq components of the series current. The voltages $V_1\angle\theta_1$and $V_2\angle\theta_2$ are the shunt and series voltage magnitudes and angles, respectively. V_{dc} is the voltage across the dc capacitor, R_{dc} represents the switching losses, R_{S1} and L_{S1} are the shunt transformer resistance and inductance, respectively, and $R_{s2}$and L_{S2} are the series transformer resistance and inductance, respectively. The control parameters$K_1(K_2)$ and$\propto_1 (\propto_2)$are, respectively, the modulation gain and voltage phase angle of the shunt (series) injected voltage. The power balance equations at bus 1 (sending) are:

$$0=V_1((i_{d1} - i_{d2})\cos\theta_1 + (i_{q1} - i_{q2})\sin\theta_1) - V_1\sum_{j=1}^{n} V_j Y_{1j} \quad (15)$$

$$0=V_1((i_{d1} - i_{d2})sin\theta_1 - (i_{q1} - i_{q2})\cos\theta_1) - -V_1\sum_{j=1}^{n} V_j\, Y_{1j} \quad (16)$$

And at bus 2 (receiving)

$$0=V_2\left(i_{d2}\cos\theta_2 + i_{q2}\sin\theta_2\right) - V_2\sum_{j=1}^{n} V_j Y_{2j}\cos(\theta_2-\theta_j-\varphi_{2j}) \quad (17)$$

$$0=V_2\left(i_{d2}\,sin\,\theta_2 + i_{q2}\,cos\,\theta_2\right) - V_2\sum_{j=1}^{n} V_j Y_{2j}\,sin(\theta_2-\theta_j-\varphi_{2j}) \quad (18)$$

Figure 7 shows a power injection model of the UPFC. The series branch shows the series injected voltage and the shunt branch with voltage controlled by k_1 and $\propto_1$. Combining (10)-(18) yields nine equations with thirteen unknowns; therefore, additional constraints are necessary to fully determine the operating equilibrium. In the power injection model, three parameters may be arbitrarily set: the shunt bus voltage magnitude and the series active and reactive powers such that:

$$P_{SC} = V_{d2}i_{d2}+V_{Q2}i_{q2} \quad (19)$$

$$Q_{sc} = V_{q2}i_{d2}-V_{d2}i_{q2} \quad (20)$$

Where V_{sc}, P_{SC} andQ_{sc} are the specified desired values. The schematic representation of the UPFC is shown in Figure 8 [21], [22]. It consists of two voltage source converters and a dc circuit represented by the capacitor. Converter 1 is primarily used to provide the real power demand of converter 2 at the common dc link terminal from the ac power system. Converter 1 can also generate or absorb reactive power at its ac terminal, which is independent of the active power transfer to (or from) the dc terminal. Therefore, with proper control, it can also fulfill the function of an independent advanced static VAR compensator providing reactive power compensation for the transmission line and thus executing indirect voltage regulation at the input terminal of the UPFC. Converter 2 is used to generate a voltage source at the fundamental frequency with variable amplitude ($0 \le V_T \le V_{Tmax}$ and phase angle $0 \le \varphi_T \le 2\pi$, which is added to the ac transmission line by the series-connected boosting transformer. The inverter output voltage injected in series with line can be used for direct voltage control, series compensation, phase shifter, and their combinations. This voltage source can internally generate or absorb all the reactive power required by the different type of controls applied and transfers active power at its dc terminal. The equivalent circuit of UPFC placed in line-connected between bus- and bus- is shown in Fig. 9. UPFC has three controllable parameters, namely, the magnitude and the angle of inserted voltage (V_T, φ_T) and the magnitude of the current (I_q).

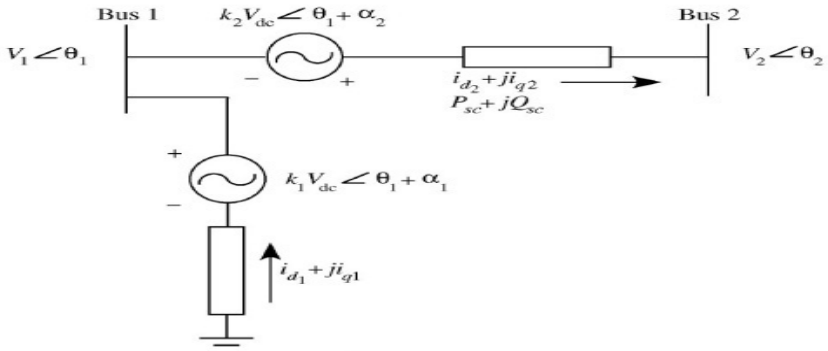

Figure 7. UPFC equivalent model

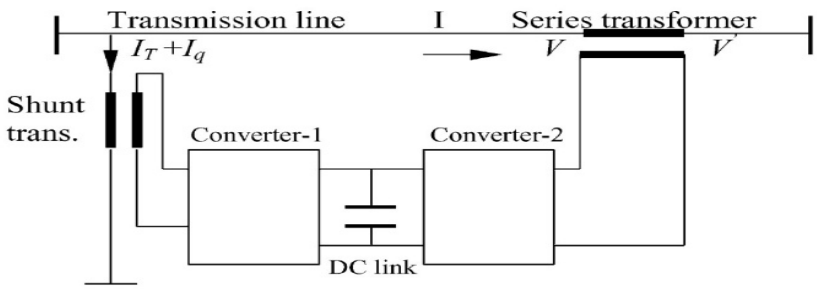

Figure 8. Schematic diagram of UPFC

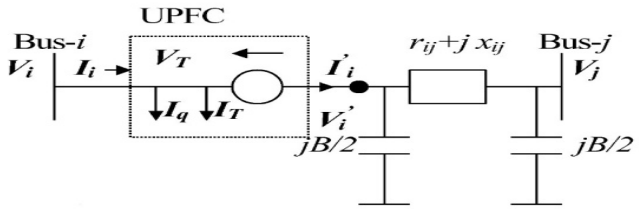

Figure 9. Equivalent circuit of UPFC

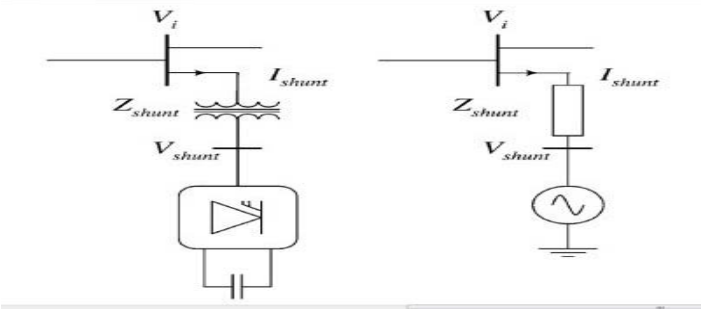

Figure 10. AC-side representation of shunt elements

Based on the principle of UPFC and the vector diagram, the basic mathematical relations can be given as:

$$V'_i = V_i + V_T \text{ , } Arg(I_q) = Arg(V_i) \pm \pi/2$$
$$Arg(I_T) = Arg(V_i) \quad \text{and} \quad I_T = \frac{Re[V_T I_i^{'*}]}{V_i} \tag{21}$$

The power flow equations from bus-*i* to bus-*j* and from bus-*j*to bus-*i* can be written as:

$$S_{ij} = P_{ij} + jQ_{ij} = V_i I_{ij}^* = V_i(\frac{jV_iB}{2} + I_T + I_q + I_i^{'})^* \tag{22}$$

$$S_{ji} = P_{ji} + jQ_{ji} = V_j I_{ji}^* = V_i(\frac{jV_jB}{2} - I_i^{'})^* \tag{23}$$

Active and reactive power flows in the line having UPFC can be written, with (21)-(23), as:

$$P_{ij} = (V_I^2 + V_T^2)g_{ij} + 2V_iV_Tg_{ij}\cos(\varphi_t - \delta_i) - V_jV_T[g_{ij}\cos(\varphi_t - \delta_j) + b_{ij}\,sin(\varphi_t - \delta_i)] -$$
$$V_iV_j(g_{ij}cos\delta_{ij} + b_{ij}sin\delta_{ij}) \tag{24}$$

$$Q_{ij} = -V_iI_q - V_i^2\left(b_{ij} + {}^{B}/_{2}\right) - V_iV_T\left[g_{ij}\,sin(\varphi_t - \delta_i) +\right.$$
$$\left.(b_{ij} + {}^{B}/_{2})\cos(\varphi_t - \delta_j)\right] - V_iV_j(g_{ij}sin\delta_{ij} - b_{ij}cos\delta_{ij}) \tag{25}$$

References [23]-[25] discuss the harmonic-domain representation of pulse width-modulated (PWM) converters and their application to the unified power-flow controller (UPFC). The UPFC can be modeled at harmonic frequencies by considering two PWM switching spectra and their interaction on both the ac and dc sides of the converter.

2.1. PWM Converter Representation

Since power-electronic converters are, in principle, switching modulators, they can be characterized in terms of the harmonic transfers between the ac and dc sides. This implementation reduces the storage requirements for each harmonic phasor by recognizing the conjugated nature of negative frequency terms. Each harmonic phasor is therefore a complex vector of length *nh*, the highest harmonic of interest. These harmonic phasors are transferred across a converter via convolution with the converter's positive frequency spectra (s_{ph}) of bandwidth 2*nh* (fulfilling the Nyquist rate). The transfers can therefore be described as:

$$\boldsymbol{V_{acph}} = \boldsymbol{V_{dcph}} \otimes s_{ph} \quad (26)$$

$$\boldsymbol{I_{dc}} = \sum_{\boldsymbol{ph=1}}^{\boldsymbol{3}} \boldsymbol{I_{ac}} \otimes s_{ph} \quad (27)$$

Where bold text refers to a harmonic phasor, *ph* refers to phase quantities, and ⊗ represents Smith's positive frequency convolution. The PWM spectra s_{ph} are described as a function of the switching instants, each of which is defined by classical PWM theory. The switching instants are stored in a vector φ , which contains an ON and OFF instant for each of the N_p conduction periods. The individual instants are calculated with a single variable Newton scheme at the beginning of each iteration. The result is the PWM switching spectra, which is defined at the *h* th harmonic as:

$$S_h = \sum_{p=1}^{N_p} \frac{j}{2\pi} (\varphi OFF_P - \varphi ON_P),\ h=0 \quad (28)$$

$$S_h = \sum_{p=1}^{N_P} \frac{(e^{jh\varphi ON_P} - e^{j\varphi OFF_P})}{\pi} \quad (29)$$

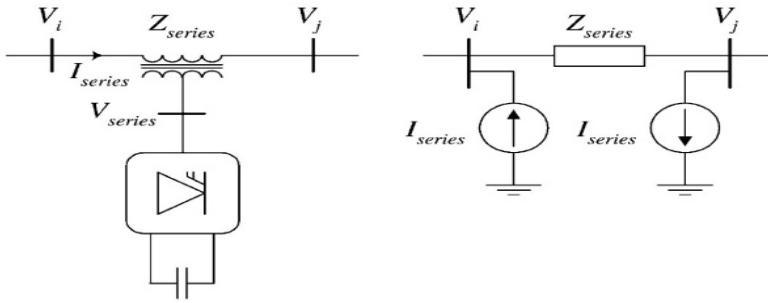

Figure 11. AC-side representation of series elements

2.2. Shunt and Series Connections

Since FACTS devices use predominantly voltage source conversion, it is convenient and logical to include shunt converters as harmonic voltage sources (Figure 10). This approach, unlike shunt current injection models, does not require knowledge about the terminal voltage (V_i) to make the voltage source substitution. This logic does not extend to series converters where, in order to avoid voltage dependence problems, it is more concise to use a pair of opposing shunt current sources (Figure 11). This representation is possible since the injected current can be defined in terms of the converter voltage and transformer leakage impedance (z_{Series})both of which are known:

$$I_{Series} = \frac{V_{Series}}{Z_{Series}} \quad (30)$$

This representation maintains the generality of the solution format, allowing the UPFC to be modeled by combining a shunt and series representation. It is important to note that these models are only used to formulate the harmonic mismatches, a conventional dual voltage source representation being used within the power flow.

2.3. AC-Side Harmonic Interaction

Since the interaction between the series and shunt equivalent circuits is assumed to occur across a predominantly linear network, they are easily combined using traditional circuit analysis First consider the system admittance matrix, which has been partitioned into sub matrices *A* –J , according to the type of harmonic injection present at each busbar.

$$\begin{bmatrix} I_{VSource} \\ I_{IHarm} \\ I_{VHarm} \end{bmatrix} = \begin{bmatrix} A & B & C \\ D & E & F \\ G & H & J \end{bmatrix} \times \begin{bmatrix} V_{VSource} \\ V_{IHarm} \\ V_{VHarm} \end{bmatrix} \quad (31)$$

Where $V_{VSource}$ refers to ideal voltage-source busbars (e.g., the voltage source component of the system equivalent V_{inf}), $V_{IHarm}$the voltage at harmonic current injection busbars (V_i and V_j in Figure 12), and V_{VHarm} the harmonic voltage-source busbars (V_{shunt} in Figure 11). All other busbars (e.g., load busbars) are treated as harmonic current injection busbars with the harmonic injection set to zero. By assuming that no voltage harmonics are present at the ideal voltage sources, it is possible to describe the unknown current flows (I_{VHarm}) at the harmonic voltage source busbars and the unknown voltages (V_{IHarm}) at the harmonic current injection busbars:

$$\begin{aligned} I_{VHarm} &= [HE^{-1}]I_{IHarm} + [J - HE^{-1}F]V_{VHarm} \\ V_{JHarm} &= [E^{-1}]I_{IHarm} - [E^{-1}F]V_{VHarm} \end{aligned} \quad (32)$$

These effectively describe the harmonic interaction between any number of harmonic voltage or current sources used to represent FACTS devices. The mathematical UPFC model was derived with the aim of being able to study the relations between the electrical transmission system and UPFC in steady-state conditions [26]. The basic scheme of this model is shown in Figure 12.This figure represents a single-line diagram of a simple transmission line with a resistance, an inductive reactance, a UPFC, a sending-end voltage source $\overline{V_S}$, and a receiving-end voltage source $\overline{V_r}$, respectively. According to Figure 13, the currents $\overline{I_S}, \overline{I_\iota}$ and$\overline{I_r}$ are calculated by the following expressions:

$$\overline{I_s} = \frac{1}{X_{eq}^2}\left(V_i e^{j\delta_i}(r_2 + jX_2) + jV_r X_i - V_S e^{j\delta}\left(r_2 + j(X_2 + X_i)\right) - V_b e^{j\delta_b}\left(r_2 + j(X_2 + X_i)\right)\right) \quad (33)$$

$$\overline{I_\iota} = \frac{1}{X_{eq}^2}\left(-V_b e^{j\delta_b}(r_2 + jX_2) - V_r(r_1 + jX_1) - V_S e^{j\delta}(r_2 + jX_2) - V_i e^{j\delta_i}\left(r_1 + r_2 + j(X_1 + X_2)\right)\right) \quad (34)$$

$$\overline{I_r} = \frac{1}{X_{eq}^2}\left(-V_i e^{j\delta_i}(r_1 + jX_1) - jV_s e^{j\delta_i}X_i - jV_b e^{j\delta_b}X_i - V_r\left(r_1 + j(X_1 + X_i)\right)\right) \quad (35)$$

Where,

$$X_{eq}^2 = X_1X_2 + (X_1 + X_2)X_i - jr_2(X_1 + X_i) - r_1\left(r_2 + j(X_2 + X_i)\right) \quad (36)$$

Figure 14 shows the single-line diagram of a UPFC connected at the end of the transmission line. The vector diagram of an UPFC connected to a network (Figure 13) is presented in Figure 14. According to Figure 15, $V_{bP}$and $V_{bq}$are the components of the series voltage of UPFC. They are proportional to the voltage at the point of connection of UPFC and can be written as:

$$V_{bq} = V_r\beta(t) \;\; and \quad V_{bp} = V_r\gamma(t) \quad (37)$$

Where $\beta(t)$ and $\gamma(t)$ are the control variables. Neglecting network losses, the electrical power can be expressed as:

$$P_r = \frac{E'V_1}{X}\sin(\delta - \theta) = \frac{E'V_1}{X}(sin\delta cos\theta - cos\delta sin\theta) \quad (38)$$

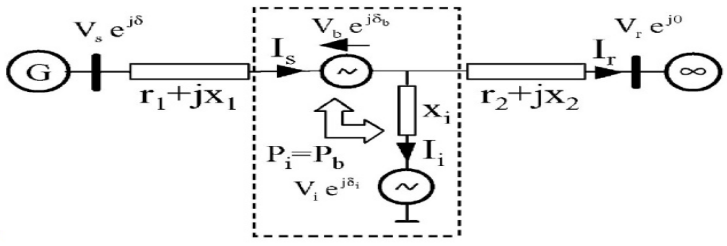

Figure 12. Mathematical model of a UPFC installed in a transmission line

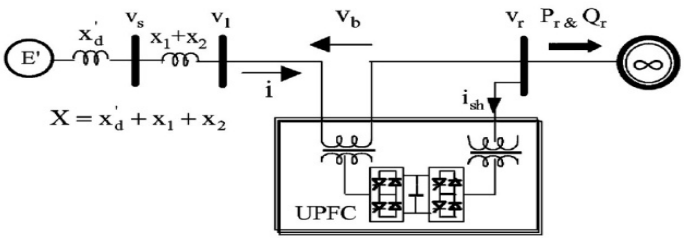

Figure 13. Generator-infinite bus system with the UPFC

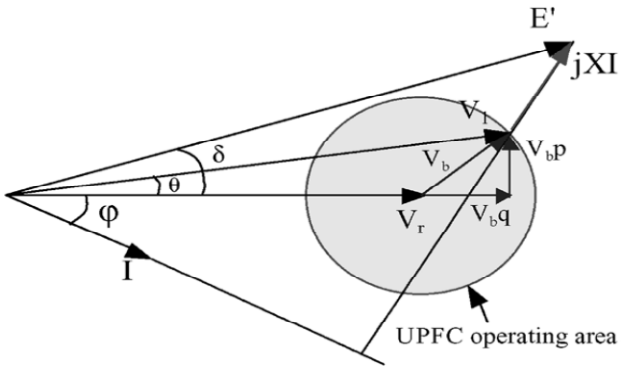

Figure 14. Vector diagram of a UPFC connected to a network

Where X is the equivalent transient reactance which includes the transient reactance of generator, the reactance of the transformer and the transmission line. The generator swing equation is:

$$M\,{}^{d^2}/_{dt^2} = P_m - Asin(\delta) - D\frac{d\delta}{dt} - P_{UPFC} \quad (39)$$

Where:

$$A = \frac{E'V_r}{X} \quad and \quad P_{UPFC} = -Acos\,(\delta)\gamma(t) + \text{Asin}(\delta)\beta(t) \quad (40)$$

Where P_{UPFC} introduces additional damping to the system if it is positive and proportional to the speed deviation $\frac{d\delta}{dt}$. This can be achieved through the following control strategy:

$$\gamma(t) = -Kcos(\delta)\frac{d\delta}{dt} \quad and\ \beta(t) = Ksin(\delta)\frac{d\delta}{dt} \quad (41)$$

By replacing (41) in (40), the damping factor is D_{UPFC} represented as below:

$$P_{UPFC} = KA\frac{d\delta}{dt} = D_{UPFC}\frac{d\delta}{dt}. \quad (42)$$

According to Figure 15, there are the following equations:

$$V_r + V_{bq} + XIsin(\varphi) = E'\cos\,(\delta) \quad (43)$$

$$V_{bp} + XIcos(\varphi) = E'\sin\,(\delta) \quad (44)$$

Then:

$$P_r = \frac{V_r E'}{X}\sin(\delta) - \frac{V_r V_{bP}}{X} \quad (45)$$

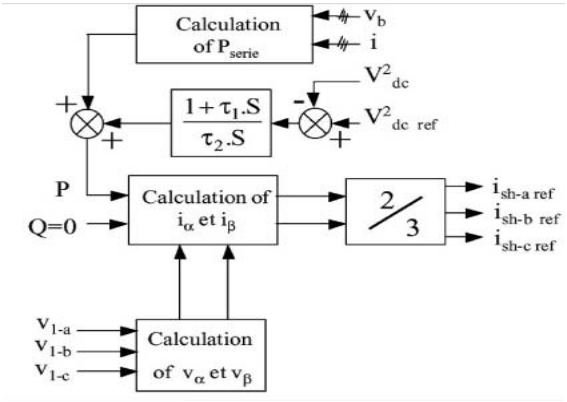

Figure 15. Control block diagram of a STATCOM

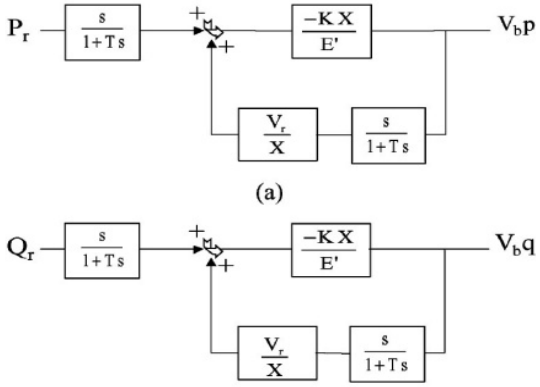

Figure 16. Modulation controller for Vp and Vq

$$Q_r = \frac{V_r E'}{X}\cos(\delta) - \frac{V_r V_{bq}}{X} - \frac{V_r^2}{X} \quad (46)$$

The partial derivative of P_r is calculated as:

$$\frac{dP_r}{dt} = \frac{\partial P_r}{\partial \delta} \times \frac{d\delta}{dt} + \frac{\partial P_r}{\partial V_{bP}} \times \frac{d(V_{bp})}{dt} = \frac{(-V_{bP})E'}{KX} - \frac{V_r}{X} \times \frac{d(V_{bp})}{dt} \quad (47)$$

The partial derivative of $Q_r$is also calculated as:

$$\frac{dQ_r}{dt} = \frac{\partial Q_r}{\partial \delta} \times \frac{d\delta}{dt} + \frac{\partial Q_r}{\partial V_{bq}} \times \frac{d(V_{bp})}{dt} = \frac{(-V_{bP})E'}{KX} - \frac{V_r}{X} \times \frac{d(V_{bq})}{dt} \quad (48)$$

The shunt converter has two duties:

a) Control the voltage magnitude at the sending-end bus by locally generating (or absorbing) reactive power.
b) Supply or absorb real power at the dc terminals as demanded by the series converter.

The general block diagram of the shunt part control is given in Figure 16. Figure 16 shows the proposed block diagram of a modulation controller capable of producing a real differentiating element with a small time constant T. The value of K is chosen so that the injected series voltage remains at its nominal value. The values of $V_r$and $E'$are chosen as 1 p.u. The modeling of series and parallel parts of UPFC [27], [28] can be represented respectively by the following equations expressed in a d,q rotating system, which is defined such that the q component of the voltage at the second bus equals to zero (Figure 17.):

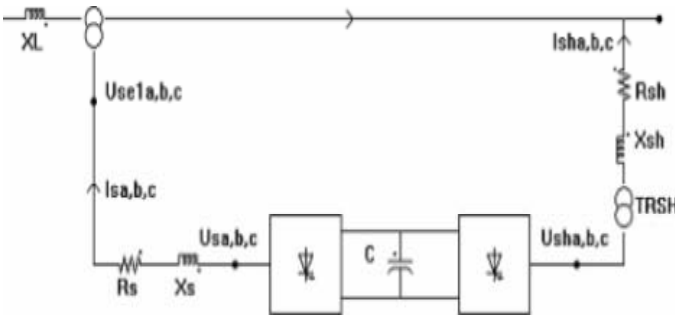

Figure 17. Simplified electric scheme of a 2-level UPFC

$$R_t I_L + L_t \frac{dI_l}{dt} + j\omega L_l L_t = U_1 - \ddot{u_{se}}.U_s - U_2 \quad (49)$$

$$R_{s\square}I_{s\square} + L_{s\square}\frac{dI_{s\square}}{dt} + j\omega L_{s\square}I_{s\square} = \frac{1}{\ddot{u_{s\square}}}U_{s\square} - U_2 \quad (50)$$

$$R_t = R_l + \ddot{u_{se}^2}R_s, L_t = L_l + \ddot{u_{se}^2}L_{se} \quad (51)$$

$\ddot{u_{se}}$and $\ddot{u_{sh}}$ represent respectively the voltage ratios of the series and parallel transformers. The transfer functions related to these two equations expressed in per unit and represented in the Laplace domain are given in Table 1.

Table 1. Type Sizes for Papers

SERIES PART	SHUNT PART
$G_S(s) = \frac{\frac{1}{r_t}}{1 + (s + j\omega)T_t}$ Whit $T_t = \frac{l_t}{r_t}$	$G_S(s) = \frac{\frac{1}{r_{s\square}}}{1 + (s + j\omega)T_{sh}}$ Whit $T_{s\square t} = \frac{l_{s\square}}{r_{sh}}$

3. CONCLUSION

The paper has presented different models of UPFC in some papers in recent years. Steady-state, dynamic, mathematical model, UPFC control model, harmonic domain UPFC model of unified power flow controller (UPFC) reported in this paper.

REFERENCES

[1] Radu, Daniel, Yvon Besanger. A multi-objective genetic algorithm approach to optimal allocation of multi-type FACTS devices for power systems security. *Power Engineering Society General Meeting, IEEE.* 2006.

[2] N.G.Hingorani. *Power electronics in electrical utilities: role of power electronics in future power systems. Proc*. of the IEEE. 1988; 76(4): 481-482.

[3] Enrique Acha. FACTS Modelling and Simulation in Power Networks. 2004 John Wiley & Sons Ltd

[4] EH Miller Damping Performance Analysis of IPFC and UPFC controllers using validated Small-Signal Models. *IEEE Trans. IEEE Trans. Power* Delivery. 2011; 26(1): 446–454.

[5] Rajabi Ghahnavieh, M Fotuhi-Firuzabad, M Shahidehpour, R Feuillet. UPFC for Enhancing Power System Reliability). *IEEE Transactions on Power Delivery*. 2010; 25(4): 2881-2889.

[6] SR Samantaray, LN Tripathy, PK Dash. Differential equation –based fault locator for unified power flow controller-based transmission line using synchronised pharos Measurements. *IET Gener. Transm. Distrib.,* 2009; 3(1): 86–98.

[7] YH Song, AT Johns. Flexible AC Transmission Systems (FACTS), ser. *IEE Power and Energy Series 30*. London, U.K. Inst. Elec. ENG. 1999.

[8] MH Haque. Evaluation of First Swing Stability of a Large Power System with Various FACTS Devices. *IEEE Trans. Power Syst.*, 2008; 23(3): 11441151.

[9] L Gyugyi. *Unified power-flow control concept for flexible ac transmission systems.* Proc. Inst. Elect. Eng. C,. 1992; 139(4): 323–331.

[10] L Gyugyi, CD Schauder, SL Williams, TR Rietman, DR Torgerson, A Edris. The unified power-flow controller: A new approach to power transmission control. *IEEE Trans. Power Del.*, 1995; 10(2): 1085-1093.

[11] MH Haque. *Application of UPFC to enhance transient stability limit.* Proc. IEEE Power Eng. Soc. General Meeting, Tampa, FL. 2007; 24–28.

[12] V Azbe, U Gabrijel, D Povh, R Mihalic. The energy function ofa general multimachine system with a unified power flow controller. *IEEE Trans. Power Syst.*, 2005; 20(3): 1478-1485.

[13] M Noroozian, L Angquist, M Ghandhari, G Andersson. Improving power system dynamics by series-connected FACTS devices,"*IEEE Trans. Power Del.*, 1997; 12(4): 1635–1641.

[14] F Aminifar, M Fotuhi-Firuzabad, R Billinton. Extended reliability model of a unified power flow controller. *IET Gener. Transm. Distrib.,* 2007; 1(6): 896–903.

[15] Billinton R, Fotuhi Firuzabad M, Faried SO, Aboreshaid S. Impact of unified power flow controllers on power system reliability. IEEE Trans. Power Syst., 2000: 15: 410–415.

[16] Fotuhi Firuzabad M, Billinton R, Faried SO, Aboreshaid S. *Power system reliability enhancement using unified power flowcontrollers*. Proc. IEEE Int. Conf. on Power System Technology. 2000: 745–750.

[17] Billinton R, Fotuhi Firuzabad M, Faried SO, Aboreshaid S. *Power system adequacy evaluation incorporating a unified power flow controller*. Proc. Conf. on Electrical and Computer Engineering, Canada. 2001; 363–368.

[18] Billinton R, Fotuhi Firuzabad M, Faried SO. Power system reliability enhancement using a thyristor controlled series capacitor. *IEEE Trans. Power Syst.,* 1999; 14: 369–374.

[19] M Zarghami, ML Crow. The Existence of Multiple Equilibria in the UPFC Power Injection Model. *IEEE Trans. Power Syst.*, 2007; 22(4): 2280–2282.

[20] L Dong, et al. A reconfigurable FACTS system for university laboratories. *IEEE Trans. Power Syst.*, 2004; 19(1): 120-128.
[21] JY Liu, YH Song, PA Mehta. Strategies for handling UPFCconstraints in the steady state power flow and voltage control. *IEEETrans. Power Syst.*, 2000; 15(2): 566–571.
[22] JY Liu, YH Song. Comparison studies of unified power flowcontroller with static var compensators and phase shifters. *Elect. Mach.Power Syst.*, 1999; 27: 237–251.
[23] KS Verma, HO Gupta. Impact on Real and Reactive Power Pricing in Open Power Market Using Unified Power Flow Controller. *IEEE Trans. Power Syst.*, 2006; 21(1): 365–371.
[24] A Wood, C Osauskas. A linear frequency-domain model of a STATCOM. *IEEE Trans. Power Del.*, 2004; 19(3): 1410–1418.
[25] Christopher Collins, Neville Watson, Alan Wood. UPFC Modeling in the Harmonic Domain. *IEEE Trans. Power Del*. 2006; 21(2): 933-938.
[26] Eskandar Gholipour, Shahrokh Saadate. Improving of Transient Stability of Power Systems Using UPFC. *IEEE Trans. Power Del.*, 2005; 20(2): 1677–1682.
[27] I Papic, P Zunko, D Povh, M Weinhold. Basic control of Unified Power Flow Controller. *IEEE Transactions on Power Systems*, 1997; 12(4): 1734-1739.
[28] M Zadehbagheri, Naziha Ahmad Azli. Performance Evaluation of Custom Power Devices in Power Distribution Networks to Power Quality Improvement: A Review. *InterInternational Journal of Scientific & Engineering Research*. 2013; 4(5). ISSN 2229-5518.

BIOGRAPHIES OF AUTHORS

Mahmoud Zadehbagheri was born in Yasouj, Iran in October 1979. In 2003 he received his B.S. in Electrical Engineering from Kashan University and in 2008 he received his M.S. in Electrical Engineering from the Islamic Azad University, Najafabad Branch, he is currently pursuing your PhD at Sabzevar university. He is with the faculty of the Electrical Engineering Department, Islamic Azad University of Yasouj. His research interests include the fields of power electronics, electrical machines and drives, FACTS devices and Power Quality.

Rahim Ildarabadi was born in Sabzevar, Iran in 1975. He received the PhD degree from Ferdowsi University of Mashhad in 2010. He is a full time faculty member at Sabzevar Hkim Sabzevari University. His main area of interest are automation system, electrical machine derive, renewable energy, instruments and measurement. He is currently an Assistant Professor of electrical engineering at Hakim SabzevariUniversity.

Majid Baghaei Nejad received the B.S. and M.Sc degree in electrical engineering from Ferdowsi University, and Tarbiat Modares University, Iran, in 1996 and 2000 respectively, and his PhD degree in electronic and computer systems from Royal Institute of Technology (KTH), Stockholm, Sweden in 2008. Since 2000 he has been with electronics department at Hakim Sabzevari University, Iran, where currently has an assistance professor position. His current research work includes low power analog/RF integrated circuit design, ultra wideband communication, RFID systems and wireless sensing.